



Published in final edited form as:

*Mucosal Immunol.* 2009 September ; 2(5): 450–461. doi:10.1038/mi.2009.95.

## Non-equilibrium and differential function between intraepithelial and lamina propria virus-specific TCR $\alpha\beta$ <sup>+</sup> CD8 $\alpha\beta$ <sup>+</sup> T cells in the small intestinal mucosa

D Isakov<sup>1,3</sup>, A Dzutsev<sup>1,3</sup>, IM Belyakov<sup>1,2</sup>, and JA Berzofsky<sup>1</sup>

<sup>1</sup> Molecular Immunogenetics and Vaccine Research Section, Vaccine Branch, Center for Cancer Research, National Cancer Institute (NCI), National Institutes of Health (NIH), Bethesda, Maryland, USA

<sup>2</sup> Midwest Research Institute, Frederick, Maryland, USA

### Abstract

The gastrointestinal mucosa regularly encounters commensal and pathogenic microbiota. Gut mucosal lymphocytes consist of two phenotypically different populations residing in the intestinal intraepithelial (IEL) compartment and lamina propria (LP). Little is known about compositional and functional differences of antigen-specific T cells from these mucosal compartments after mucosal infection, or the degree of trafficking between them. We here studied the B8R<sub>20–27</sub>-specific CD8 T-cell response in LP and IEL compartments after intrarectal immunization with modified vaccinia virus Ankara (MVA). CD8<sup>+</sup> T cells in the IEL compartment had much lower avidity than in the LP or spleen during acute and memory phases. Surprisingly, the TCR V $\beta$ -chain distribution of antigen-specific T cells and the length of the CDR3 region of the dominant V $\beta$  genes showed substantial dissimilarities between IEL and LP antigen-specific CD8 $\alpha\beta$  T cells in individual mice, increasing with time. We show functional and compositional differences between these mucosal compartments during the effector and memory phases of the immune response, indicating limited crosstalk and microenvironmental differences between the IEL, LP, and spleen. The restricted migration of cells from each of these mucosal compartments could partly account for a founder effect we observed in the IEL TCR $\alpha\beta$  CD8 $\alpha\beta$  epitope-specific repertoire that might impact protective efficacy.

### INTRODUCTION

It is well known that protective immunity in the small intestine is accomplished by lymphoid cells present both in scattered IELs and LP and organized formations (Peyer's patches and mesenteric lymph node, overall known as the gut-associated lymphoid tissue).<sup>1,2</sup> In these formations, there are inductive sites (Peyer's patches) where priming takes place and effector sites (IEL and LP), where effector antigen-specific T cells reside. In the vast majority of available publications, the role of a particular compartment of gut-associated lymphoid tissue was studied after oral inoculation of pathogens, and in substantially fewer of them, after intrarectal (IR) administration of antigens/viruses.<sup>3–12</sup> The small bowel has been shown to be a major site of human immunodeficiency virus replication.<sup>13</sup> We have also previously shown that protection against simian/human immunodeficiency virus correlated with the frequency and avidity of antigen-specific cells residing in the LP of the small intestine.<sup>4,14,15</sup> An effective strategy for the development of a vaccine depends on

Correspondence: IM Belyakov (igorbelyakov@yahoo.com).

<sup>3</sup>These authors contributed equally to this work.

knowledge of the natural route of infection and the route of administration of the vaccine, as well as on the formulation of the vaccine itself (peptide, adjuvants, DNA, recombinant replication-competent/incompetent virus).<sup>16–18</sup> In several studies, it was shown that IR administered vaccinia virus vectors or human immunodeficiency virus type-1 peptide vaccines elicited development of antigen-specific memory CD8<sup>+</sup> T cells, associated with lymphoid tissues in the gut (LP and Peyer's patches),<sup>19</sup> were effective in the presence of pre-existing anti-poxvirus immunity,<sup>20</sup> and provided protection after mucosal challenge.<sup>19,21</sup> In further unpublished observations, we also found that IR immunization with vaccinia virus induces a much stronger memory immune response in IEL and LP than oral or subcutaneous immunizations. The mucosal vaccines induced a higher percentage of functionally active interferon (IFN)- $\gamma$ -producing antigen-specific CD8<sup>+</sup> T cells in the gut mucosa in mice and macaques.<sup>15</sup> In addition, our recent study showed that in macaques infected with simian/human immunodeficiency virus, the preservation of CD4<sup>+</sup> T cells in colonic LP and the reduction of simian/human immunodeficiency virus load in the intestine correlated better with the presence of high-avidity mucosal cytotoxic T lymphocytes.<sup>15</sup>

Previous studies have examined the naive T-cell repertoire in these compartments.<sup>22,23</sup> We here showed for the first time the distribution of antigen-specific CD8<sup>+</sup> T cells with different functional avidities in the small intestinal mucosa after IR administered MVA, and the TCR V $\beta$ -chain usage and CDR3 length distribution of these cells isolated at the effector and memory phases from the spleen, as well as small intestinal IEL and LP, after infection/vaccination. CD8<sup>+</sup> T cells with a high functional avidity were remarkably enriched *in vivo* in the LP but significantly decreased in the intraepithelial compartment after IR immunization in the same individual mouse. The TCR V $\beta$ -chain usage and CDR3 length distribution of antigen-specific CD8<sup>+</sup> cytotoxic T lymphocyte also revealed substantial dissimilarities between these mucosal compartments. This approach might be useful to evaluate and improve the efficacy of vaccines based on attenuated poxviruses, whether for smallpox or for other diseases in which a recombinant antigen, such as human immunodeficiency virus gp 160, is inserted into the recombinant vaccinia vector.<sup>24–27</sup> The results also show that despite the close anatomic proximity of the compartments, the antigen-specific TCR $\alpha\beta$ <sup>+</sup> CD8 $\alpha\beta$ <sup>+</sup> T cells in the IEL and LP are not in equilibrium with each other after infection or vaccination.

## RESULTS

### Kinetics and activity of CD8<sup>+</sup> T-cell responses after mucosal viral infection

To study the crosstalk between intraepithelial and LP TCR $\alpha\beta$ <sup>+</sup> CD8 $\alpha\beta$ <sup>+</sup> T cells in the small intestinal mucosa, we immunized C57BL/6 mice IR with MVA at a dose of 10<sup>7</sup> PFU. By using B8R<sub>20–27</sub>/H-2K<sup>b</sup> tetramer, we were able to measure the kinetics of CD8<sup>+</sup> T-cell expansion and contraction in the spleen, IEL, and LP compartments. As shown by flow cytometry analysis during the effector phase of infection (7 days post-infection), the IR route of infection elicited robust expansion of B8R<sub>20–27</sub>/H-2K<sup>b</sup> tetramer<sup>+</sup> CD8<sup>+</sup> T cells in the LP and the IEL (Figure 1a), representing 24.9±7.02 and 16.5±4.7% of CD8<sup>+</sup> T cells, respectively ( $P > 0.05$ ). In the spleen, the magnitude of the response was lower, giving rise to only 9.7±3.5% of CD8<sup>+</sup> T cells (spleen vs. IEL,  $P > 0.05$ ; spleen vs. LP,  $P < 0.01$ ). In contrast, during the memory phase (2 months after immunization), the relative percentages of B8R<sub>20–27</sub>/H-2K<sup>b</sup> tetramer<sup>+</sup> CD8<sup>+</sup> T cells were almost equal in all tested compartments, indicating that the degree of contraction of antigen-specific cells was much lower in the spleen than in LP or IEL (Figure 1b). When the functional activity of these cells was tested by ELISpot assay, it was found to have a different pattern. The total number of IFN- $\gamma$ -producing cells was almost the same ( $P > 0.05$ ) in all tested compartments during the acute phase (Figure 1c), but significantly reduced in mucosal sites during the memory phase (Figure 1d). The difference between the total number of antigen-specific T cells stained with

tetramer (Figure 1a and b) and the number of T cells producing cytokine (Figure 1c and d) suggests the regulation of the functional activity. Reduction in the numbers of cells capable of producing IFN- $\gamma$  in the gut could be an important physiologic mechanism protecting the intestine from collateral cytokine damage that may develop after bystander activation of locally residing memory CD8 T cells. Such a mechanism may be of special importance for the gut, as it is considered to be not only a shock organ, but also a place where immune cells are being constantly activated by the food as well as microfloral antigens.

### Differences in functional avidity among compartments

Previously, it was found that during the memory phase of MVA infection, the functionally active antigen-specific CD8<sup>+</sup> T cells could be detected after IR vaccination in both LP and IEL compartments.<sup>28</sup> However, the functional avidity vs. the number of antigen-specific CD8<sup>+</sup> T cells of adjacent IEL and LP during infection has not been studied yet. To estimate this, we performed an ELISpot assay for IFN- $\gamma$  production with directly *ex vivo* isolated cells from the spleen, IEL, and LP at the effector and memory phases. Functional avidity was defined by the response to different peptide concentrations, known to be dependent on multiple factors, that, besides the intrinsic affinity of the T-cell receptor, also include other factors, such as the expression of co-stimulatory receptors and the efficiency of signal transduction.<sup>14,29–34</sup> As the magnitude of IFN- $\gamma$  production in these compartments was quite different, to compare the shapes of dose–response curves for IFN- $\gamma$ -producing cells of IEL, LP, and spleen, we normalized the dose–response data obtained by IFN- $\gamma$  ELISpot to a common scale. By normalizing raw ELISpot data during both the effector and the memory phases of infection, we observed that B8R<sub>20–27</sub>-specific CD8<sup>+</sup> T cells residing in the LP were of much higher avidity than cells from IEL compartment ( $P < 0.001$ ) as shown on Figure 2a and b. Interestingly, antigen-specific cells in the LP were also of higher avidity than those in the spleen ( $P < 0.05$ ). Surprisingly, the most dramatic differences between cells from the spleen and LP were found not for the cells responding to the highest peptide concentration (1  $\mu$ M), but for those recognizing the lowest one (1 pM), which became even more profound at 2 months after vaccination.

To visualize the direct contribution of subsets with different functional avidities to the total IFN- $\gamma$  production, we recalculated the ELISpot data, given that the measured responders to the lowest concentration of peptide that induces detectable response represent the actual (net) numbers of cells with high avidity (1 pM), and the measured number of responders to the nearest higher concentration is a sum of both actual (net) responders to that concentration and responders to the next lower concentration (e.g., net 100pM responders = measured 100pM responders – 1pM responders, see Methods section). Figure 2c and d displays normalized net values. We observed that the cells with different avidity comprise the bulk of the B8R<sub>20–27</sub>-specific IFN- $\gamma$ -producing cells for each compartment during the acute and memory phases of infection. During the acute phase of infection (Figure 2c), the dominant population of splenocytes responded to 100pM of B8R<sub>20–27</sub> peptide, whereas the dominant population in the LP compartment responded to both 1 and 100 pM, and that of the IEL compartment responded to 1  $\mu$ M. During the memory phase (Figure 2d), the largest fraction of splenocytes responded to 100 pM, that of LP cells to 1pM, and that of IEL to 1  $\mu$ M. Thus, we conclude that during both acute and memory phases of the immune response, the majority of B8R<sub>20–27</sub>-specific CD8<sup>+</sup> T cells in the LP have high functional avidity, in the spleen, intermediate avidity, and in the IEL, low avidity. It is important to note that CD8<sup>+</sup> T cells from anatomically adjacent IEL and LP compartments have approximately three-log difference in the optimal peptide concentration required for their activation. We speculate that such a dramatic difference in the functional avidity of the cells between LP and IEL compartments could be a consequence of a long-lasting restriction in the recirculation of antigen-specific T cells between the two compartments, allowing the

cells to be exposed to microenvironmental factors that affect functional avidity and IFN- $\gamma$  production in IEL, and not to migrate into LP and vice versa.

### Distinct TCR repertoires among compartments

To test our hypothesis, we analyzed the TCR V $\beta$ -chain usage by B8R<sub>20-27</sub>-specific CD8<sup>+</sup> T cells from the IEL, LP, and spleen, which would allow us to tell whether our data on functional avidity reflect the consequence of a restriction in antigen-specific cell migration or some other factors.

Previously, it was reported that the intraepithelial and LP CD8 $\alpha\beta$ <sup>+</sup> TCR $\alpha\beta$ <sup>+</sup> T cells of the small intestine compared within individual naive mice contain the identical T-cell clones in contrast to the peripheral lymphoid organs, indicating that the two mucosal compartments easily exchange T cells between them,<sup>22</sup> but immune or infected mice were not studied. Even though antigen-specific CD8 T cells represent a fraction of CD8 $\alpha\beta$  TCR $\alpha\beta$  cells, different mechanisms that mediate their initial localization inside these compartments may significantly affect their migratory properties in immunized/infected vs. naive mice. By using a panel of antibodies against different TCR V $\beta$  chains, we estimated their relative usage by B8R<sub>20-27</sub>/H-2K<sup>b</sup> tetramer<sup>+</sup> CD8 $\beta$ <sup>+</sup> T cells from the spleen, IEL, and LP for each individual mouse ( $n = 8$ ) during the acute and memory phases. Owing to the paucity of memory antigen-specific CD8 T cells recovered after isolation from the LP 2 months after immunization, we could not analyze V $\beta$ -chain distribution in this compartment. So far, no data have been published describing the TCR V $\beta$ -chain repertoire of immunodominant B8R<sub>20-27</sub>-specific CD8<sup>+</sup> T cells.

We found that during the acute phase of infection, the dominant B8R-specific clones isolated from the spleen were positive for V $\beta$ 2, -8.1, -11, and -13, whereas during the memory phase, V $\beta$ 8.1/8.2 and -8.3 dominated. Interestingly, during both the acute and memory phases of MVA infection, mean values of the distributions for different TCR V $\beta$  chains in the spleen, IEL, and LP were similar for most of the V $\beta$  chains studied (Figure 3). We also noted that in sharp contrast to the acute phase, the V $\beta$ -chain usage profoundly changed during the memory phase, a phenomenon similar to that previously described for a number of other epitopes.<sup>35</sup> More surprising was to find the much greater variation of V $\beta$ -chain usage among individual mice in the IEL compartment as compared with the spleen during the memory phase, shown as much greater s.d. bars (compare Figure 3a and b). To further analyze these data, we measured the magnitude of variability among values (spread or variance of the distribution) in the expression of TCR V $\beta$ -chain profile among tissues, which is estimated as the coefficient of variation (CV) (CV was calculated by dividing values of s.d. by the values of mean, multiplied by 100%; Figure 3c and d). Such breadth or variance of the distribution would not be expected to correlate with the magnitude of the response. The higher the CV is, the greater the variance in the sample is. As we can see from Figure 3c and d, the variation of V $\beta$ -chain usage in B8R-specific IEL between individual mice increased significantly over time. In contrast, the CV for V $\beta$ -chain usage of B8R-specific cells isolated from the spleen did not change with time or was slightly reduced. Such an increase of CV of V $\beta$ -chain usage in IEL may suggest an influence of some unknown mechanism(s) favoring a stochastic distribution of different T-cell clones. There are a few possibilities that may help explain this phenomenon: (1) it is possible that only a limited number of T-cell clones survive/remain in the small intestine during the memory phase resulting in a founder effect, or (2) it might happen that different commensal microflora strains present in different mice drive expansion of different T-cell clones. However, despite the reason for such a stochastic pattern for V $\beta$ -chain distribution in the IEL, which is not seen in the spleen, it may also suggest a lack of T-cell recirculation between the spleen and IEL. Similar conclusions regarding limiting recirculation of cells from gut mucosa through central lymphoid tissues were drawn elsewhere.<sup>36</sup>

To further elucidate dissimilarities in V $\beta$ -chain profile found in different tissues, we made a pairwise comparison of V $\beta$ -chain distribution between different compartments for each mouse (Figure 4). Interestingly, no significant correlation of V $\beta$ -chain usage ( $P > 0.05$ ) between any compartments was found during either the acute or the memory phase of infection (except for the V $\beta$ 13 chain, acute phase, IEL vs. LP,  $P < 0.05$ , which is in fact even not significant if one corrects it for the number of V $\beta$ s tested, a further indication of very little T-cell recirculation between tested compartments). Interestingly, such anatomically close compartments as IEL and LP of the small intestine showed that B8R-specific CD8<sup>+</sup> T-cell clones are distributed in a dissimilar way when mice were analyzed individually.

We also compared the V $\beta$  profile of the total CD8 $\beta$ -positive IEL and LP cells and found that even though the overall profiles of the V $\beta$ -chain usage for the cells from IEL and LP were different between tetramer-positive T cells and total T cells, some similarities were still present, such as a high percent of V $\beta$ 2-positive T cells (data not shown). Also, we did not observe significant differences in the V $\beta$ -chain usage between LP and IEL in the non-antigen-specific total population of CD8 $\beta$ <sup>+</sup> T cells, concordant with earlier reports.<sup>23</sup>

To further characterize B8R-specific CD8<sup>+</sup> T cells from IEL and LP compartments, we analyzed the length of the CDR3 region of the TCR genes by the immunoscope method. We isolated IEL and LP cells at different time points and sorted B8R tetramer<sup>+</sup> CD8<sup>+</sup> cells using the FACS Aria Cell-Sorting System. In all,  $2 \times 10^4$  cells were collected from each organ during the acute phase of infection and  $5 \times 10^3$  cells during the memory phase for analysis. RNA was isolated from each sample and used as a template for the cDNA synthesis. The cDNA was amplified with primers specific for each V $\beta$  gene (BV) and for the C $\beta$  (constant region of the TCR gene, abbreviated as BC) and the BV-BC PCR product was analyzed using ABI Prism 377 and GeneMapper software. The profile of CDR3 length for dominant V $\beta$ -chain genes (Figure 5) of the B8R-specific CD8<sup>+</sup> T cells in all tested samples was highly irregular, indicative of the oligoclonal composition of the B8R-specific T cells in both compartments, and is consistent with the well-known oligoclonality for epitope-specific T cells. At both time points, we also observed differences between CDR3 length profiles for cytotoxic T lymphocyte from the IEL and LP, which is reflected by differences in the presence and height of individual peaks. Significantly more differences between IEL and LP compartments were observed during the memory phase. The most unexpected observation was the much higher degree of oligoclonality exhibited by IEL B8R-specific T cells during the memory phase (Figure 5), as compared with LP B8R-specific T cells. We have to note that the total number of B8R tetramer-positive CD8<sup>+</sup> T cells per LP or IEL compartment was approximately the same (data not shown). We also used an equal number of the cells per organ per analysis, and therefore, the observed reduction in the size of the clonal population of the T cells cannot be explained by a reduction in the numbers of the antigen-specific T cells in the IEL compartment or in the sample studied. Therefore, these large differences in the usage of T-cell clones in neighboring compartments in the gut imply the existence of different mechanisms responsible for the maintenance of the effector–memory T cells in the IEL and LP.

To sum up, B8R-specific CD8<sup>+</sup> T cells from all tested compartments are compositionally and functionally different, probably developing independently and having a limited crosstalk among them. Significant differences in the functional avidity of IEL, LP lymphocytes (LPL), and spleen CD8<sup>+</sup> T cells may also be explained by microenvironmental differences (such as cytokines, chemokines, intrinsic antigen-presenting capacity of parenchymal vs. blood-derived antigen-presenting cells) in those compartments.

## Migratory capacity of IEL

A question that arose from our study was as follows: what would be the physiologic function for such a restricted migration of IEL T cells to and from other compartments? Does it represent a consequence of limited migratory abilities or is it linked to their capacity to survive outside the IEL compartment? To test this, we isolated CD8<sup>+</sup> T cells from the IEL and spleen of naive donor wild-type (WT) animals, labeled them with different fluorescent markers, mixed them together, and transferred them into naive WT recipient mice. CD8<sup>+</sup> IELs did not efficiently migrate back to the IEL compartment (Figure 6a), but rather migrated to the spleen (Figure 6b) or lung (Figure 6c). Interestingly, the level of migration of donor IEL to the recipient IEL compartment was even lower than that for splenocytes. We assumed that one of the reasons for the lack of donor IEL migration back to the IEL compartment could be a competition with resident lymphocytes. Therefore, we transferred carboxyfluorescein succinimidyl ester-labeled CD8<sup>+</sup> IELs or CD8<sup>+</sup> splenocytes from naive WT animals into naive severe combined immunodeficiency mice, which lack T cells in all tissues including the gut. We found that CD8<sup>+</sup> IELs not only lack the ability to efficiently migrate to the IEL compartment, but are also unable to survive in any other site outside the small intestinal mucosa even in the lymphopenic hosts (Figure 6d–f), in contrast to transferred splenic CD8<sup>+</sup> T cells. Among the transferred IELs, only half had the CD8 $\alpha\beta$ <sup>+</sup> TCR $\alpha\beta$ <sup>+</sup> phenotype, whereas the rest of the CD8 $\alpha$ <sup>+</sup> cells were composed of CD8 $\alpha\alpha$ <sup>+</sup> TCR $\alpha\beta$ <sup>+</sup> and CD8 $\alpha\alpha$ <sup>+</sup> TCR $\gamma\delta$ <sup>+</sup> T cells. However, even taking these numbers into account, the differences between IEL and spleen observed on Figure 6a–f were between 10- and 500-fold, which exceed the potential bias introduced by different phenotypes of CD8 $\alpha$ <sup>+</sup> T cells in IEL vs. spleen. Similar data were obtained when migration of adoptively transferred CD8<sup>+</sup> T cells from IEL was studied during the acute phase of vaccinia virus infection in recipient mice (data not shown). Thus, these results imply the existence of different mechanisms by which CD8<sup>+</sup> T cells from IEL and spleen survive. We suggest that the restricted potential of CD8<sup>+</sup> IELs to migrate outside the gut mucosa could help to preserve the long-term antigen-specific CD8<sup>+</sup> T cells in IEL and/or LP compartments during the memory phase of viral infection.

## DISCUSSION

The capacity of mucosal antigen-specific CD8<sup>+</sup> T cells to be protective *in vivo* was shown in several papers after adoptive transfer of either total or CD8 $\alpha\beta$ <sup>+</sup> TCR $\alpha\beta$ <sup>+</sup> IEL subsets.<sup>37–40</sup> It is also known that LP and IEL compartments contain long-lasting functional antigen-specific CD8<sup>+</sup> T cells.<sup>19,41</sup> Previously, it was shown that isolated IEL or LP subsets stimulated directly *ex vivo* with antigen could produce modest-to-high amounts of IFN- $\gamma$ <sup>42–44</sup> or kill target cells pulsed with antigen.<sup>19,41,44,45</sup> However, no direct comparison of these subsets was made. To address this question, we used MVA virus, which, due to the abortive replication cycle, expresses viral antigens for a very short period of time, and the IR route of infection to directly target the development of antigen-specific CD8<sup>+</sup> T cells to the gut.<sup>46</sup> By using B8R<sub>20–27</sub>/H-2K<sup>b</sup> tetramer staining for flow cytometry, we estimated the kinetics of expansion and contraction of CD8 $\alpha\beta$ <sup>+</sup> TCR $\alpha\beta$ <sup>+</sup> T cells in the spleen, IEL, and LP compartments in the small intestine. We found that the degree of contraction of B8R tetramer<sup>+</sup>-positive CD8<sup>+</sup> cells isolated from LP or IEL was higher than that in the spleen. In contrast, when we estimated functional activity of cells, we found that during both the effector and the memory phases of infection, the number of total IFN- $\gamma$ -producing cells was the highest in the spleen followed by the LP, and was the lowest in the IEL. When we measured antigen-specific IFN- $\gamma$  production during the memory phase of infection, we also found that the magnitude of response to B8R peptide was disproportionately low in the IEL compartment when compared with the high number of B8R tetramer-positive cells found

there. Previously, reduced IFN- $\gamma$  production in IEL was also described,<sup>43</sup> although not so profoundly as we found in our study.

To further study functional differences of antigen-specific CD8<sup>+</sup> T cells between mucosal compartments and the spleen, we analyzed the functional avidity of the cells by measuring IFN- $\gamma$  production at different peptide concentrations by ELISpot assay. To our knowledge, the distribution of cells with different functional avidities in the small intestinal mucosa has never been previously examined. We found a dramatic difference in avidity between B8R-specific CD8<sup>+</sup> T cells from IEL and LP, an unexpected finding given that the two compartments are adjacent to each other. In particular, CD8<sup>+</sup> T cells with a high functional avidity were remarkably enriched in the LP after IR administered viruses, which is of special importance, because the presence of high-avidity cells is strongly correlated with protective immunity.<sup>14,17,29,30,31,47–49</sup> Perhaps, such hyporesponsiveness of SI-IEL with regard to IFN- $\gamma$  production may have a protective role due to a number of detrimental effects of this cytokine on specific functions of different types of intestinal epithelial cells,<sup>50–54</sup> which, being unleashed, may lead to pathologic conditions.<sup>55</sup>

As in quantitative and qualitative terms these two mucosal compartments of the small intestine were so dissimilar, we suggested that, at least in part, it might be explained by a lack of free recirculation of antigen-specific CD8 T cells between IEL and LP. This assumption was tested by comparing the TCR V $\beta$ -chain profile present on B8R<sub>20–27</sub>/H2-K<sup>b</sup> tetramer<sup>+</sup> CD8<sup>+</sup> T cells in the two compartments. We reasoned that if little or no migration existed between IEL and LP, we might observe differences in V $\beta$ -chain usage. Previously, little difference was found in total SI-IEL cells vs. lymphocytes from peripheral lymph nodes in naive mice, but the question was never examined in antigen-specific T cells in immune or infected mice.<sup>22,23</sup> We evaluated the dynamics for TCR V $\beta$ -chain-bearing cells among B8R<sub>20–27</sub>/H-2K<sup>b</sup> tetramer<sup>+</sup> CD8 $\alpha\beta$ <sup>+</sup> TCR $\alpha\beta$ <sup>+</sup> T cells from the IEL, LP, and the spleen. During the acute phase of the infection, we found that cells from both the spleen as well as the gut had a rather broad TCR V $\beta$ -chain profile, characterized by the presence of cells expressing several dominant and subdominant V $\beta$  chains (Figure 3). The dominant TCR V $\beta$  chains found in the acute phase in all compartments tested were V $\beta$ 2, -8.1/8.2, and -13. We also observed that during the memory phase, the pattern of dominant V $\beta$  chains changed and became narrower, in agreement with previously published data,<sup>35</sup> where a difference in V $\beta$ -chain usage was observed between effector and memory CD8 T cells for Epstein–Barr virus epitopes in humans. However, this may not always be the case, and may depend on the pathogen and species studied.<sup>56</sup>

More interesting data were obtained when we compared the degree of V $\beta$ -chain variation in the IEL compartment among individual mice during the memory phase: it turned out to be much higher than for the spleen, which is a strong indication that the IELs are not recirculating through central lymphoid tissues. Moreover, if cells from the same tissues were compared among different mice, even more striking disparities in the usage of TCR V $\beta$  chains were found. Similarly, mainly random TCR V $\beta$ -chain usage by antigen-specific CD8 $\alpha\beta$ <sup>+</sup> TCR $\alpha\beta$ <sup>+</sup> T cells from the spleen compared with IEL and LP was previously described during the effector phase of *Listeria monocytogenes* infection in mice.<sup>57</sup> Interestingly, such an uneven distribution of T-cell clones between mucosal compartments and peripheral lymphoid tissues was described earlier in naive mice,<sup>22</sup> where individual inbred mice displayed distinct and apparently non-overlapping oligoclonal repertoires of CD8 $\alpha\beta$  TCR $\alpha\beta$  IEL as compared with the cells from peripheral lymphoid tissues. On the other hand, in naive mice IEL and LP were found to have identical clones (an indication of efficient cell exchange between compartments). To test whether that is the case for the antigen-specific CD8<sup>+</sup> T cells after a mucosal infection, we used a similar approach and analyzed the V $\beta$ -chain profile of B8R-specific T cells in the spleen, IEL, and LP. By

analyzing V $\beta$  usage of B8R-specific CD8 T cells in these compartments for individual mice, we found no correlation between any pair of these compartments ( $P < 0.05$ , two-way analysis of variance test and Student's  $t$ -test). Therefore, we concluded that cell exchange between the mucosal compartments was not enough to provide for the presence of identical clones; however, we are aware that our data did not address the presence of such recirculation directly.

More direct evidence of that was obtained when we analyzed the length of the CDR3 region of the TCR genes. We found significant differences in the profile of the CDR3 region of antigen-specific cells in IEL and LP as early as 7 days post-infection, and therefore, the overall clonal composition of these two compartments must be different as well. The largest differences in the clonal composition of IEL and LP were found at day 60 post-infection, suggesting again the existence of a clonal "drift" over time between compartments with limited crosstalk. We also observed much greater oligoclonality in B8R tetramer-positive cells in IEL during the memory phase, when compared with LP. A similar oligoclonality among IEL was also reported in the total CD8<sup>+</sup> population after colonization of germ-free mice.<sup>58</sup> However, the estimation of total clones of T cells (not specific for a particular antigen) residing in LP and IEL usually reveals less dramatic differences between compartments, counting approximately 250 clones for IEL and 350 for LP.<sup>23,58</sup> However, the same studies indicated more similarities between the T cells from the IEL and LP compartments, rather than their differences. Such discrepancies between earlier published studies and our data could be attributed to the nature of our immunogen (virus vs. bacteria). A more likely possible explanation is that the current study is the first to report the dynamics of the diversity of antigen-specific T cells during acute and memory phases in the gut, which is a different scenario from the relatively steady-state situation in the gut, when most of the antigens (food or bacteria) are constantly present. The clear tendency of the vaccinia-specific IEL to show a high degree of oligoclonality could reflect differences in the effector T-cell maintenance in the IEL and LP compartments, possibly involving sudden loss of a large proportion of the IEL T cells followed by immediate expansion of the remaining cells or by a founder effect in the IEL, when only few cells can get into the IEL compartment, but once there, they rapidly expand. Notably, the total number of the antigen-specific T cells per organ was not decreased, which indicates that narrowing of the clonal repertoire of the B8R-specific T cells is not related to an overall reduction in the population size of the IEL.

Although the mechanisms underlying this uneven TCR V $\beta$ -chain and CDR3 distribution on antigen-specific CD8<sup>+</sup> T cells in mucosal vs. lymphoid tissues are not known yet, we addressed the possible reasons for such a limited recirculation between these compartments. For this, we modeled a situation in which IEL cells would have been forced to recirculate back to the IEL compartment in naive recipient animals after IELs from naive donors were adoptively transferred. When naive or acutely infected recipient WT mice were hosting CD8<sup>+</sup> T cells from donor mice mucosally infected with vaccinia virus, a very poor ability of IEL to migrate back into IEL or LP compartments was observed. Moreover, a very poor ability to survive outside the IEL compartment was seen, in contrast to transferred splenocytes. Thus, we speculate that if IEL had easily migrated out of this compartment, these cells would not have been able to migrate back without antigen stimulation and would most likely have undergone apoptosis, suggesting that IELs would have rapidly lost their memory CD8 T-cell population. Similar results were also seen in previous parabiosis studies in mice,<sup>36</sup> where memory CD8<sup>+</sup> IEL failed to reach equilibrium between parabiotic mice. Various factors may play a role in the restriction of free migration of antigen-specific CD8<sup>+</sup> IEL from their original compartment, including chemokines and integrins. It is known that IELs express both  $\alpha 4\beta 7$  and CCR9,<sup>59,60</sup> which guide the migration of cells to the gut mucosa. A potentially important factor explaining the lack of T-cell recirculation found by



us and others<sup>36</sup> could be an inability of IEL to survive outside IEL compartment (see Figure 6d and e). Further studies will be pursued to solve this question.

Overall, our data indicated that there is a surprising lack of equilibrium between the antigen-specific CD8 $\alpha\beta$ <sup>+</sup> TCR $\alpha\beta$ <sup>+</sup> T cells in the LP and epithelial compartments of the intestine after mucosal viral infection/vaccination. This lack of equilibrium is supported functionally by a drastic difference in apparent functional avidity of the specific T cells, and phenotypically by distinct TCR V $\beta$  usage among cells specific for the same immunodominant peptide–MHC complex, determined by tetramer staining and by the distinct CDR3 profiling of CD8<sup>+</sup> tetramer<sup>+</sup> T cells. We also observed a striking variation in V $\beta$  usage among epitope-specific CD8<sup>+</sup> IELs in individual mice. This stochastic pattern suggests a founder effect in which a limited number of precursors are responsible for populating the epithelial compartment. This founder effect also supports the lack of interchange between the IEL and LP compartments. Such a stochastically determined limited repertoire among IEL may lead to a significant mouse-to-mouse variation in immune responses/protective efficacy of the IEL.

## METHODS

### Mice

Female C57BL/6 mice were purchased from the Frederick Cancer Research Center (Frederick, MD). Female severe combined immunodeficiency mice were purchased from Jackson Laboratories (Bar Harbor, ME). All studies were carried out under protocols approved by the NCI Animal Care and Use Committee.

### Virus and immunization protocol

Replication-incompetent vaccinia virus strain MVA, originally from A Mayr, University of Munich, Germany,<sup>61,62</sup> was a gift from Drs Bernard Moss, Patricia Earl, and Linda Wyatt (NIAID).<sup>63</sup> This virus was propagated and titered in chicken embryo fibroblast cells. For immunization, mice were IR injected with MVA 10<sup>7</sup> PFU.

### Cell purification: isolation of small intestinal intraepithelial and LP lymphocytes, and lymphocytes from the spleen

Spleens were aseptically removed and single-cell suspensions were prepared by a gentle passage of the tissue through sterile screens. Erythrocytes were lysed with Tris-buffered ammonium chloride and the remaining cells were washed extensively in RPMI-1640 (Gibco, Invitrogen Corporation, Grand Island, NY) containing 2 % fetal bovine serum (Gibco, Invitrogen Corporation, Grand Island, NY).

To prepare IEL in mice, intestines from killed mice were removed, flushed with RPMI-1640, and visible PPs were cut out.<sup>64</sup> The intestines were longitudinally opened and washed with cold RPMI-1640. The intestines were then cut into 1-cm pieces, placed into a flask, and shaken with a magnetic stirrer in 20 ml of Dulbecco's phosphate-buffered saline (PBS) containing 4mM EDTA (PHOENIX Biotechnologies, Huntsville, AL) and 1mM dithiothreitol (Thermo Fisher Scientific Inc., Rockford, IL) for 40 min at 37 °C. The supernatant was filtered through a 70- $\mu$ m cell strainer (BD Falcon, Bedford, MA). IELs were isolated on 10 ml Lympholyte-M cell separation media (Cedarlane Laboratories Limited, Hornby, Ontario, Canada) by centrifugation for 30 min at 2,000 r.p.m. For isolation of LP, the intestinal pieces from which IEL had been recovered were digested in 5 ml RPMI-1640 (Gibco, Invitrogen Corporation, Grand Island, NY) containing 10% fetal bovine serum (Gibco, Invitrogen Corporation, Grand Island, NY), 100 $\mu$ gml<sup>-1</sup> penicillin–streptomycin solution (Mediatech Inc., Manassas, VA), 2mM L-glutamine (Mediatech), 80Uml<sup>-1</sup> collagenase type VIII, and 200  $\mu$ gml<sup>-1</sup> DNase I (Sigma-Aldrich Corp., St Louis,

MO) for 40 min at 37 ° C. The LPL were then isolated on Lympholyte M similarly as for IEL cells.

### Flow cytometry and cell sorting

Lymphocytes were resuspended in staining buffer (PBS, 1% bovine serum albumine) at a concentration of  $10^7$  cells per ml and incubated at 4 ° C with Fc-Block (PharMingen, San Diego, CA) for 15 min. After that, samples were stained with properly diluted monoclonal antibody and tetramer MHC/peptide complexes for 40 min on ice. Flow cytometry was performed using a FACScalibur, cell sorting was performed using FACSaria Cell-Sorting System, and data were analyzed with CellQuest software (Becton Dickinson, Mountain View, CA) and FlowJo 8.5 (Tree Star, Ashland, OR). The following monoclonal antibodies were used: PerCP-conjugated anti-CD8 $\alpha$  (clone 53-6.7; obtained from PharMingen) and allophycocyanin-conjugated anti-CD8 $\beta$  (clone CT-CD8b; obtained from eBiosciences, San Diego, CA). Soluble tetrameric B8R<sub>20-27</sub>/H-2K<sup>b</sup> complex was conjugated to phycoerythrin-labeled streptavidin (made by the NIH Tetramer Core Facility). Expression by B8R<sub>20-27</sub>/H-2K<sup>b</sup> tetramer<sup>+</sup> CD8<sup>+</sup> T cells of different TCR V $\beta$  chains was determined using a Mouse V $\beta$  TCR Screening Panel according to the manufacturer (fluorescein isothiocyanate-conjugated monoclonal antibodies obtained from PharMingen).

### IFN- $\gamma$ ELISpot

A 96-well microtiter plate with a nitrocellulose base (Millititer HA; Millipore) was incubated overnight at 4 ° C with 100  $\mu$ l of rat anti-mouse IFN- $\gamma$  monoclonal antibody AN18 (5  $\mu$ gml<sup>-1</sup>; Mabtech Inc., Mariemont, OH) in PBS (pH 7.3). Following washing of the plate with PBS, the wells were blocked by incubation for 2 h at room temperature with complete medium (RPMI-1640 and 10% fetal calf serum). Lymphoid cells from the spleen, IEL, and LP isolated from immunized mice were placed into wells at a concentration of  $0.2 \times 10^6$  cells per well and cultured in complete media in a volume of 200  $\mu$ l per well together with directly added B8R<sub>20-27</sub> peptide (TSYKFESV), which is a dominant poxvirus cytotoxic T lymphocyte epitope restricted by H-2K<sup>b</sup>,<sup>65</sup> in ELISpot plates. The plates were incubated for at least 18 h at 37 ° C in 5% CO<sub>2</sub> and air. After that, the plates were washed thoroughly with PBS–0.05% Tween 20 (Sigma) followed by incubation with rat anti-mouse IFN- $\gamma$ -biotinylated monoclonal R4-6A2 (2  $\mu$ gml<sup>-1</sup>; Mabtech) in PBS/0.5% bovine serum albumine for 3 h at 37 ° C. After incubation with secondary monoclonal antibodies, plates were washed with PBS–0.05% Tween 20, and incubated with alkaline phosphatase substrate prepared from VECTASTAIN Elite ABC Kit (Vector Laboratories) for 1 h at room temperature. At the last stage, plates were washed with PBS–0.05% Tween 20 followed by PBS and developed with BD ELISpot AEC Substrate Set (PharMingen). Spots were counted on an AID ELISpot Reader (Cell Technology).

### RNA extraction and cDNA synthesis

Total RNA was isolated from sorted cells using Rneasy Micro Kit (Qiagen Inc., Valencia, CA) according to the manufacturer's guidelines. cDNA was prepared using RT<sup>2</sup> First Strand Kit (SuperArray Frederick, MD).

### Analyses of the TCR- $\beta$ repertoires

PCR was conducted with a set of eight different V $\beta$  primers for B8R epitope-dominant V $\beta$  genes<sup>66</sup> in combination with FAM-labeled BC primer in a volume of 50  $\mu$ l of PCR Platinum Mix (Invitrogen). BV-BC product was subsequently purified and concentrated by MinElute Purification kit (Qiagen), 35 cycles of amplification. The resultant purified product was mixed with formamide and Rox500 marker (both ABI, Foster City, CA), incubated for 5 min at 95 ° C, and analyzed using an automatic sequencer (ABI Prism 377). The data were

analyzed by GeneMapper software (ABI). The presented results are expressed as peaks corresponding to the different sizes of the PCR product ( $x$  scale) and amount (height of the peak at the  $y$  scale).

### Cell isolation, labeling, and adoptive transfers

Cells from spleen and IEL were isolated on CD8 magnetic beads according to the manufacturer's instructions (Miltenyi Biotech Inc., Auburn, CA); then dead cells were removed by using Dead Cell Removal Kit (viability > 99%; Miltenyi Biotech). After that, live CD8<sup>+</sup> IEL cells were labeled with red fluorescent linker PKH26 (Sigma-Aldrich, St Louis, MO), splenocytes—with carboxyfluorescein succinimidyl ester (1  $\mu$ M; Molecular Probes) in bovine serum albumine/Dulbecco's PBS for 15min at 37°C, mixed at a 1:1 ratio, and a total of  $5 \times 10^6$  CD8 T cells were transferred into naive C57BL/6 WT mice. Twenty-four hours later, lymphocytes were isolated from small intestine IEL and LP, large intestine IEL and LP, spleen, mesenteric lymph nodes, and lungs. (Cells from mesenteric lymph node and lungs were incubated in RPMI-1640 with fetal bovine serum containing collagenase type VIII and DNase I as for isolation of LP cells, and eventually purified on Lympholyte-M cell separation media). Then, isolated cells were analyzed by flow cytometry. For other adoptive transfer experiments, cells from naive donor C57BL/6 mice were isolated from IEL or spleen as described, labeled with carboxyfluorescein succinimidyl ester, and separately IV transferred into naive recipient severe combined immunodeficiency mice (10–12 weeks old). Seven days later, the presence of donor cells was analyzed by flow cytometry.

### Statistical analysis

All statistical analyses were performed using GraphPad Prism version 5.00, GraphPad Software (San Diego CA; www.graphpad.com). Statistical comparisons were performed using the analysis of variance and Student's  $t$ -test. Normalization of the dose-dependent IFN-gamma immune response was performed using "Normalization" function of the GraphPad Prism software.

### Acknowledgments

We thank Susan Sharrow and Larry Granger for the cell sorting. We thank Evgeny Arons for his help and valuable advice in the immunoscope analysis. We also thank Kathleen Hartman and the staff of the DNA Mimicore Facility of the NCI for genescan run. We thank Bernard Moss, Patricia Earl, and Linda Wyatt (NIAID, Bethesda, MD) for the gift of MVA and David Venzon and David Liewehr for consultation on statistical issues. We thank Dr Brian Kelsall and Dr Warren Strober for critical reading of the paper and helpful suggestions. This study was supported by the NIH intramural program of the Center for Cancer Research, NCI.

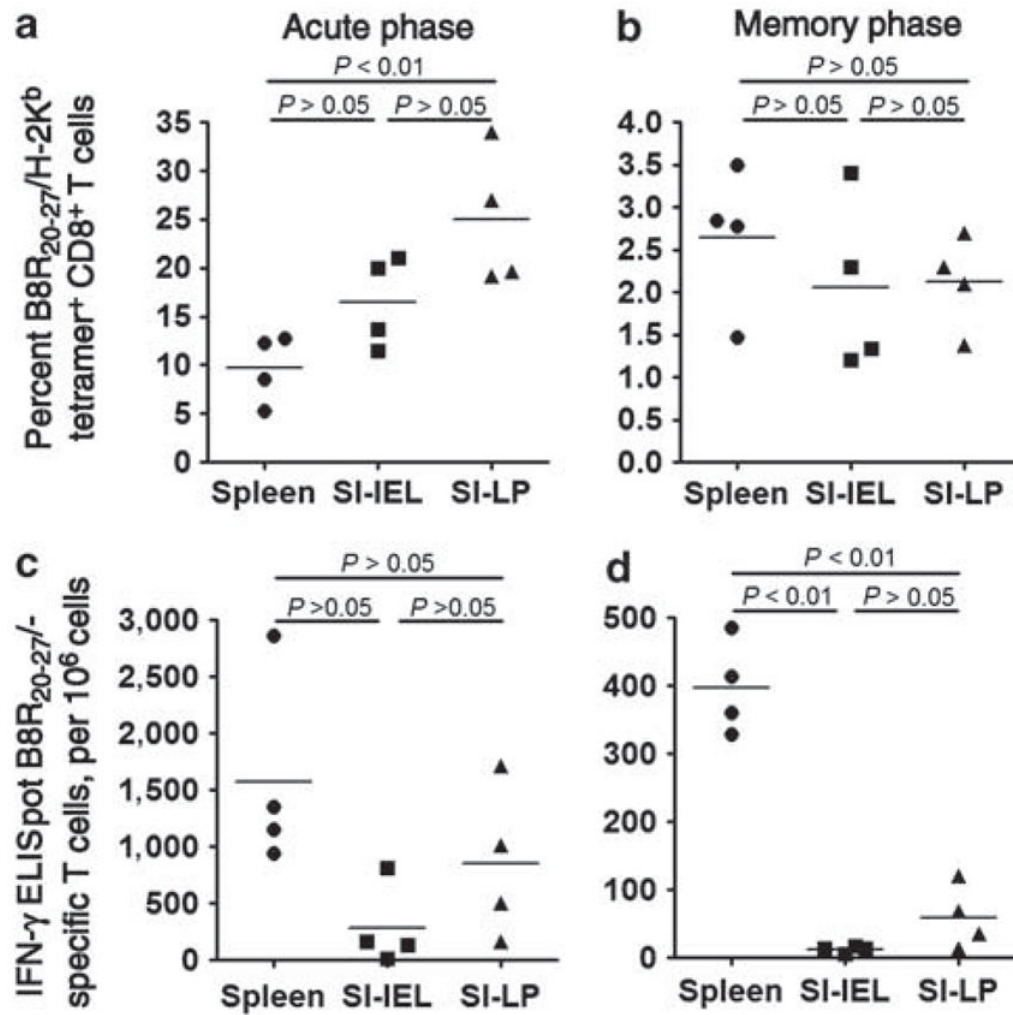
### References

1. Cheroutre H, Madakamutil L. Acquired and natural memory T cells join forces at the mucosal front line. *Nat Rev Immunol.* 2004; 4:290–300. [PubMed: 15057787]
2. Sherman MA, Kalman D. Initiation and resolution of mucosal inflammation. *Immunol Res.* 2004; 29:241–252. [PubMed: 15181286]
3. Kuznetsov VA, Stepanov VS, Berzofsky JA, Belyakov IM. Assessment of the relative therapeutic effects of vaccines on virus load and immune responses in small groups at several time points: an efficacy of mucosal and subcutaneous polypeptide vaccines in rhesus macaques exposed to SHIV. *J Clin Virol.* 2004; 31:S69–S82. [PubMed: 15567097]
4. Belyakov IM, et al. Mucosal AIDS vaccine reduces disease and viral load in gut reservoir and blood after mucosal infection of macaques. *Nat Med.* 2001; 7:1320–1326. [PubMed: 11726972]
5. Belyakov IM, Berzofsky JA. Immunobiology of mucosal HIV infection and the basis for development of a new generation of mucosal AIDS vaccines. *Immunity.* 2004; 20:247–253. [PubMed: 15030769]
6. Belyakov IM, et al. Progress on new mucosal vaccine strategies for HIV. *FASEB J.* 2004; 18:A821.

7. Kozlowski PA, Cu-Uvin S, Neutra MR, Flanigan TP. Comparison of the oral, rectal, and vaginal immunization routes for induction of antibodies in rectal and genital tract secretions of women. *Infect Immun.* 1997; 65:1387–1394. [PubMed: 9119478]
8. Kozlowski PA, Neutra MR. The role of mucosal immunity in prevention of HIV transmission. *Curr Mol Med.* 2003; 3:217–228. [PubMed: 12699359]
9. Pinczewski J, et al. Enhanced immunity and protective efficacy against SIVmac251 intrarectal challenge following ad-SIV priming by multiple mucosal routes and gp120 boosting in MPL-SE. *Viral Immunol.* 2005; 18:236–243. [PubMed: 15802969]
10. Suh YS, et al. Reduction of viral loads by multigenic DNA priming and adenovirus boosting in the SIVmac-macaque model. *Vaccine.* 2006; 24:1811–1820. [PubMed: 16274888]
11. Agnello D, et al. Intrarectal immunization with rotavirus 2/6 virus-like particles induces an antirotavirus immune response localized in the intestinal mucosa and protects against rotavirus infection in mice. *J Virol.* 2006; 80:3823–3832. [PubMed: 16571799]
12. Belyakov IM, Ahlers JD, Berzofsky JA. Mucosal AIDS vaccines: current status and future directions. *Expert Rev Vaccines.* 2004; 3 (Suppl):65–73.
13. Veazey RS, et al. Gastrointestinal tract as a major site of CD4+ T cell depletion and viral replication in SIV infection. *Science.* 1998; 280:427–431. [PubMed: 9545219]
14. Belyakov IM, et al. Impact of vaccine-induced mucosal high avidity CD8+ CTLs in delay of AIDS-viral dissemination from mucosa. *Blood.* 2006; 107:3258–3264. [PubMed: 16373659]
15. Belyakov IM, Isakov DV, Zhu Q, Dzutsev AH, Berzofsky JA. A novel functional CTL avidity/activity compartmentalization to the site of mucosal immunization contributes to protection of macaques against SHIV viral depletion of mucosal CD4+ T cells. *J Immunol.* 2007; 178:7211–7221. [PubMed: 17513770]
16. Czerkinsky C, et al. Mucosal immunity and tolerance: relevance to vaccine development. *Immunol Rev.* 1999; 170:197–222. [PubMed: 10566152]
17. Berzofsky JA, et al. Progress on new vaccine strategies against chronic viral infections. *J Clin Invest.* 2004; 114:450–462. [PubMed: 15314679]
18. Berzofsky JA, et al. Progress on new vaccine strategies for the immunotherapy and prevention of cancer. *J Clin Invest.* 2004; 113:1515–1525. [PubMed: 15173875]
19. Belyakov IM, et al. Mucosal immunization with HIV-1 peptide vaccine induces mucosal and systemic cytotoxic T lymphocytes and protective immunity in mice against intrarectal recombinant HIV-vaccinia challenge. *Proc Natl Acad Sci USA.* 1998; 95:1709–1714. [PubMed: 9465081]
20. Belyakov IM, Moss B, Strober W, Berzofsky JA. Mucosal vaccination overcomes the barrier to recombinant vaccinia immunization caused by preexisting poxvirus immunity. *Proc Natl Acad Sci USA.* 1999; 96:4512–4517. [PubMed: 10200293]
21. Belyakov IM, et al. The Importance of local mucosal HIV-specific CD8+ cytotoxic T lymphocytes for resistance to mucosal-viral transmission in mice and enhancement of resistance by local administration of IL-12. *J Clin Invest.* 1998; 102:2072–2081. [PubMed: 9854042]
22. Regnault A, Cumano A, Vassalli P, Guy-Grand D, Kourilsky P. Oligoclonal repertoire of the CD8 alpha alpha and the CD8 alpha beta TCR-alpha/beta murine intestinal intraepithelial T lymphocytes: evidence for the random emergence of T cells. *J Exp Med.* 1994; 180:1345–1358. [PubMed: 7931068]
23. Arstila T, et al. Identical T cell clones are located within the mouse gut epithelium and lamina propria and circulate in the thoracic duct lymph. *J Exp Med.* 2000; 191:823–834. [PubMed: 10755885]
24. Kwak H, et al. Improved protection conferred by vaccination with a recombinant vaccinia virus that incorporates a foreign antigen into the extracellular enveloped virion. *Virology.* 2004; 322:337–348. [PubMed: 15110531]
25. Estcourt MJ, et al. Prime-boost immunization generates a high frequency, high-avidity CD8(+) cytotoxic T lymphocyte population. *Int Immunol.* 2002; 14:31–37. [PubMed: 11751749]
26. Santra S, et al. Recombinant poxvirus boosting of DNA-primed rhesus monkeys augments peak but not memory T lymphocyte responses. *Proc Natl Acad Sci USA.* 2004; 101:11088–11093. [PubMed: 15258286]

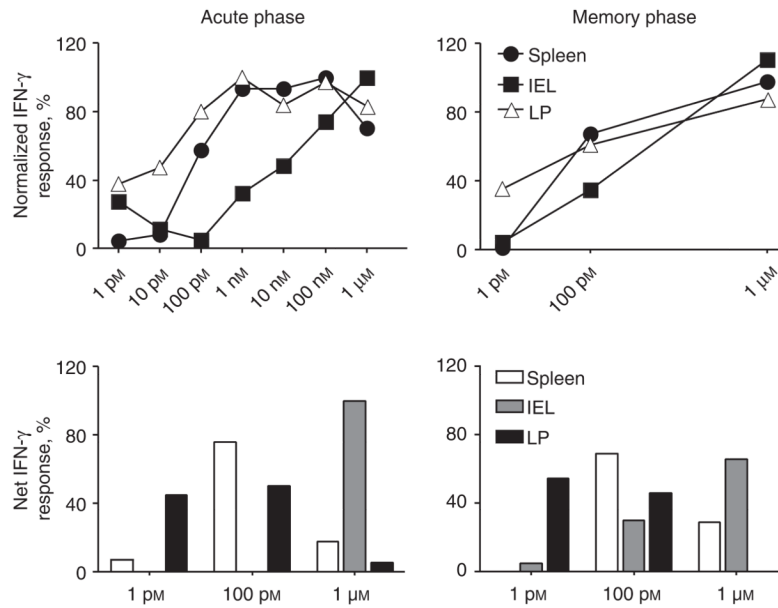
27. Vogel TU, et al. Multispecific vaccine-induced mucosal cytotoxic T lymphocytes reduce acute-phase viral replication but fail in long-term control of simian immunodeficiency virus SIVmac239. *J Virol.* 2003; 77:13348–13360. [PubMed: 14645590]
28. Belyakov IM, et al. Induction of mucosal CTL response by intrarectal immunization with a replication-deficient recombinant vaccinia virus expressing HIV 89.6 envelope protein. *J Virol.* 1998; 72:8264–8272. [PubMed: 9733870]
29. Snyder JT, Alexander-Miller MA, Berzofsky JA, Belyakov IM. Molecular mechanisms and biological significance of CTL avidity. *Curr HIV Res.* 2003; 1:287–294. [PubMed: 15046253]
30. Alexander-Miller MA, Leggatt GR, Berzofsky JA. Selective expansion of high or low avidity cytotoxic T lymphocytes and efficacy for adoptive immunotherapy. *Proc Natl Acad Sci USA.* 1996; 93:4102–4107. [PubMed: 8633023]
31. Gallimore A, Dumrese T, Hengartner H, Zinkernagel RM, Rammensee HG. Protective immunity does not correlate with the hierarchy of virus-specific cytotoxic T cell responses to naturally processed peptides. *J Exp Med.* 1998; 187:1647–1657. [PubMed: 9584143]
32. Derby MA, Alexander-Miller MA, Tse R, Berzofsky JA. High avidity CTL exploit two complementary mechanisms to provide better protection against viral infection than low avidity CTL. *J Immunol.* 2001; 166:1690–1697. [PubMed: 11160212]
33. Cawthon AG, Lu H, Alexander-Miller MA. Peptide requirement for CTL activation reflects the sensitivity to CD3 engagement: correlation with CD8alpha versus CD8alphaalpha expression. *J Immunol.* 2001; 167:2577–2584. [PubMed: 11509598]
34. Cawthon AG, Alexander-Miller MA. Optimal colocalization of TCR and CD8 as a novel mechanism for the control of functional avidity. *J Immunol.* 2002; 169:3492–3498. [PubMed: 12244138]
35. Annels NE, Callan MF, Tan L, Rickinson AB. Changing patterns of dominant TCR usage with maturation of an EBV-specific cytotoxic T cell response. *J Immunol.* 2000; 165:4831–4841. [PubMed: 11046006]
36. Klonowski KD, et al. Dynamics of blood-borne CD8 memory T cell migration *in vivo*. *Immunity.* 2004; 20:551–562. [PubMed: 15142524]
37. Moretto M, Weiss LM, Khan IA. Induction of a rapid and strong antigen-specific intraepithelial lymphocyte response during oral *Encephalitozoon cuniculi* infection. *J Immunol.* 2004; 172:4402–4409. [PubMed: 15034055]
38. McDonald V, Robinson HA, Kelly JP, Bancroft GJ. Immunity to *Cryptosporidium muris* infection in mice is expressed through gut CD4+ intraepithelial lymphocytes. *Infect Immun.* 1996; 64:2556–2562. [PubMed: 8698479]
39. Lepage AC, Buzoni-Gatel D, Bout DT, Kasper LH. Gut-derived intraepithelial lymphocytes induce long term immunity against *Toxoplasma gondii*. *J Immunol.* 1998; 161:4902–4908. [PubMed: 9794424]
40. Adjei AA, Shrestha AK, Castro M, Enriquez FJ. Adoptive transfer of immunity with intraepithelial lymphocytes in *Cryptosporidium parvum*-infected severe combined immunodeficient mice. *Am J Med Sci.* 2000; 320:304–309. [PubMed: 11093682]
41. Masopust D, Vezys V, Marzo AL, Lefrancois L. Preferential localization of effector memory cells in nonlymphoid tissue. *Science.* 2001; 291:2413–2417. [PubMed: 11264538]
42. Culshaw RJ, Bancroft GJ, McDonald V. Gut intraepithelial lymphocytes induce immunity against *Cryptosporidium* infection through a mechanism involving gamma interferon production. *Infect Immun.* 1997; 65:3074–3079. [PubMed: 9234756]
43. Masopust D, Vezys V, Wherry EJ, Barber DL, Ahmed R. Cutting edge: gut microenvironment promotes differentiation of a unique memory CD8 T cell population. *J Immunol.* 2006; 176:2079–2083. [PubMed: 16455963]
44. Belyakov IM, Ahlers JD, Clements JD, Strober W, Berzofsky JA. Interplay of cytokines and adjuvants in the regulation of mucosal and systemic HIV-specific cytotoxic T lymphocytes. *J Immunol.* 2000; 165:6454–6462. [PubMed: 11086085]
45. Lefrancois L, Olson S, Masopust D. A critical role for CD40-CD40 ligand interactions in amplification of the mucosal CD8 T cell response. *Immunol Rev.* 1999; 170:183–196. [PubMed: 10566151]

46. Ramirez JC, Finke D, Esteban M, Kraehenbuhl JP, Acha-Orbea H. Tissue distribution of the Ankara strain of vaccinia virus (MVA) after mucosal or systemic administration. *Arch Virol*. 2003; 148:827–839. [PubMed: 12721793]
47. Zeh HJ III, Perry-Lalley D, Dudley ME, Rosenberg SA, Yang JC. High avidity CTLs for two self-antigens demonstrate superior *in vitro* and *in vivo* antitumor efficacy. *J Immunol*. 1999; 162:989–994. [PubMed: 9916724]
48. Yee C, Savage PA, Lee PP, Davis MM, Greenberg PD. Isolation of high avidity melanoma-reactive CTL from heterogeneous populations using peptide-MHC tetramers. *J Immunol*. 1999; 162:2227–2234. [PubMed: 9973498]
49. Berzofsky JA, et al. Approaches to improve engineered vaccines for human immunodeficiency virus (HIV) and other viruses that cause chronic infections. *Immunol Rev*. 1999; 170:151–172. [PubMed: 10566149]
50. Adams RB, Planchon SM, Roche JK. IFN-gamma modulation of epithelial barrier function. Time course, reversibility, and site of cytokine binding. *J Immunol*. 1993; 150:2356–2363. [PubMed: 8450217]
51. Bruewer M, et al. Interferon-gamma induces internalization of epithelial tight junction proteins via a macropinocytosis-like process. *FASEB J*. 2005; 19:923–933. [PubMed: 15923402]
52. Chavez AM, Menconi MJ, Hodin RA, Fink MP. Cytokine-induced intestinal epithelial hyperpermeability: role of nitric oxide. *Crit Care Med*. 1999; 27:2246–2251. [PubMed: 10548215]
53. Leaphart CL, et al. Interferon-gamma inhibits intestinal restitution by preventing gap junction communication between enterocytes. *Gastroenterology*. 2007; 132:2395–2411. [PubMed: 17570214]
54. Tong Q, et al. Interferon-gamma inhibits T84 epithelial cell migration by redirecting transcytosis of beta1 integrin from the migrating leading edge. *J Immunol*. 2005; 175:4030–4038. [PubMed: 16148152]
55. Hue S, et al. A direct role for NKG2D/MICA interaction in villous atrophy during celiac disease. *Immunity*. 2004; 21:367–377. [PubMed: 15357948]
56. Sourdive DJ, et al. Conserved T cell receptor repertoire in primary and memory CD8 T cell responses to an acute viral infection. *J Exp Med*. 1998; 188:71–82. [PubMed: 9653085]
57. Huleatt JW, Pilip I, Kerksiek K, Pamer EG. Intestinal and splenic T cell responses to enteric *Listeria monocytogenes* infection: distinct repertoires of responding CD8 T lymphocytes. *J Immunol*. 2001; 166:4065–4073. [PubMed: 11238655]
58. Regnault A, et al. The expansion and selection of T cell receptor alpha beta intestinal intraepithelial T cell clones. *Eur J Immunol*. 1996; 26:914–921. [PubMed: 8625988]
59. Johansson-Lindbom B, et al. Selective generation of gut tropic T cells in gut-associated lymphoid tissue (GALT): requirement for GALT dendritic cells and adjuvant. *J Exp Med*. 2003; 198:963–969. [PubMed: 12963696]
60. Wiedle G, Dunon D, Imhof BA. Current concepts in lymphocyte homing and recirculation. *Crit Rev Clin Lab Sci*. 2001; 38:1–31. [PubMed: 11256516]
61. Mayr A, Hochstein-Mintzel V, Stickl H. Abstammung, eigenschaften and verwendung des attenuierten vaccinia-stammes MVA. *Infection*. 1975; 3:6–14.
62. Mayr A, Hochstein-Mintzel V, Stickl H. Origin, properties and use of the attenuated vaccina strain MVA. *Z Klin Ther Infekt*. 1987; 3:6–14.
63. Earl PL, et al. Immunogenicity of a highly attenuated MVA smallpox vaccine and protection against monkeypox. *Nature*. 2004; 428:182–185. [PubMed: 15014500]
64. Lefrancois L. Carbohydrate differentiation antigens of murine T cells: expression on intestinal lymphocytes and intestinal epithelium. *J Immunol*. 1987; 138:3375–3384. [PubMed: 2437191]
65. Tschärke DC, et al. Identification of poxvirus CD8+ T cell determinants to enable rational design and characterization of smallpox vaccines. *J Exp Med*. 2005; 201:95–104. [PubMed: 15623576]
66. Pannetier C, et al. The sizes of the CDR3 hypervariable regions of the murine T-cell receptor beta chains vary as a function of the recombined germ-line segments. *Proc Natl Acad Sci USA*. 1993; 90:4319–4323. [PubMed: 8483950]



**Figure 1.**

Expansion and contraction of B8R<sub>20-27</sub>/H2-K<sup>b</sup> tetramer<sup>+</sup> CD8<sup>+</sup> T cells in the spleen, SI-IEL, and SI-LP. Relative percentages of antigen-specific CD8<sup>+</sup> T cells after intrarectal immunization at 7 days (a) and 2 months (b) in the spleen, SI-IEL, and SI-LP are presented. Lymphocytes were isolated and stained with phycoerythrin-conjugated B8R<sub>20-27</sub>/H2-K<sup>b</sup> tetramer together with CD8 $\beta$  (SI-IEL and SI-LP) or CD8 $\alpha$  (spleen) mAbs, and analyzed by flow cytometry. Magnitude of antigen-specific IFN- $\gamma$  production at 7 days (c) and 2 months (d). Directly *ex vivo* isolated cells were *in vitro* stimulated with B8R<sub>20-27</sub> peptide (1  $\mu$ M). Number of IFN- $\gamma$  – producing cells was counted on ELISpot Reader and presented as spots per 10<sup>6</sup> cells in each tissue. Data from one of two representative experiments are shown as the mean and s.e.m. of four animals per interval. IEL, intraepithelial lymphocyte; IFN- $\gamma$ , interferon- $\gamma$ ; LP, lamina propria; mAbs, monoclonal antibodies.

**Figure 2.**

Functional avidity of B8R-specific CD8<sup>+</sup> T cell response by ELISpot for IFN- $\gamma$  production in the spleen, SI-IEL, and SI-LP. Data are normalized for comparison between compartments. Lymphocytes from the spleen and small intestine were isolated at 7 days (acute phase) and 2 months (memory phase) from the spleen, SI-IEL, and SI-LP and *in vitro* stimulated with different concentrations of B8R<sub>20–27</sub> peptide as for Figure 1c and d. (a and b) ELISpot data on the number of IFN- $\gamma$ -producing cells during acute and memory phases of MVA infection were normalized by GraphPad Prism software to a common scale. Data normalized to a common scale are shown to visualize differences in the avidity between compartments. Cells were *in vitro* stimulated with different B8R<sub>20–27</sub> peptide concentrations as described in Methods. (c and d) Normalized net ELISpot data presented as the relative percentage of cells producing IFN- $\gamma$  after *in vitro* stimulation with B8R<sub>20–27</sub> peptide. To obtain net values, ELISpot data presented on (a) and (b) were recalculated by the following formula: Net 1 pM responders = actual 1 pM responders; Net 100 pM responders = total 100 pM responders – actual 1 pM responders; Net 1  $\mu$ M responders = total 1  $\mu$ M responders – actual 100 pM responders. Data from one of two representative experiments are shown as the mean and s.e.m. of four animals per interval. IEL, intraepithelial lymphocyte; IFN- $\gamma$ , interferon- $\gamma$ ; LP, lamina propria; MVA, Modified Vaccinia Ankara.



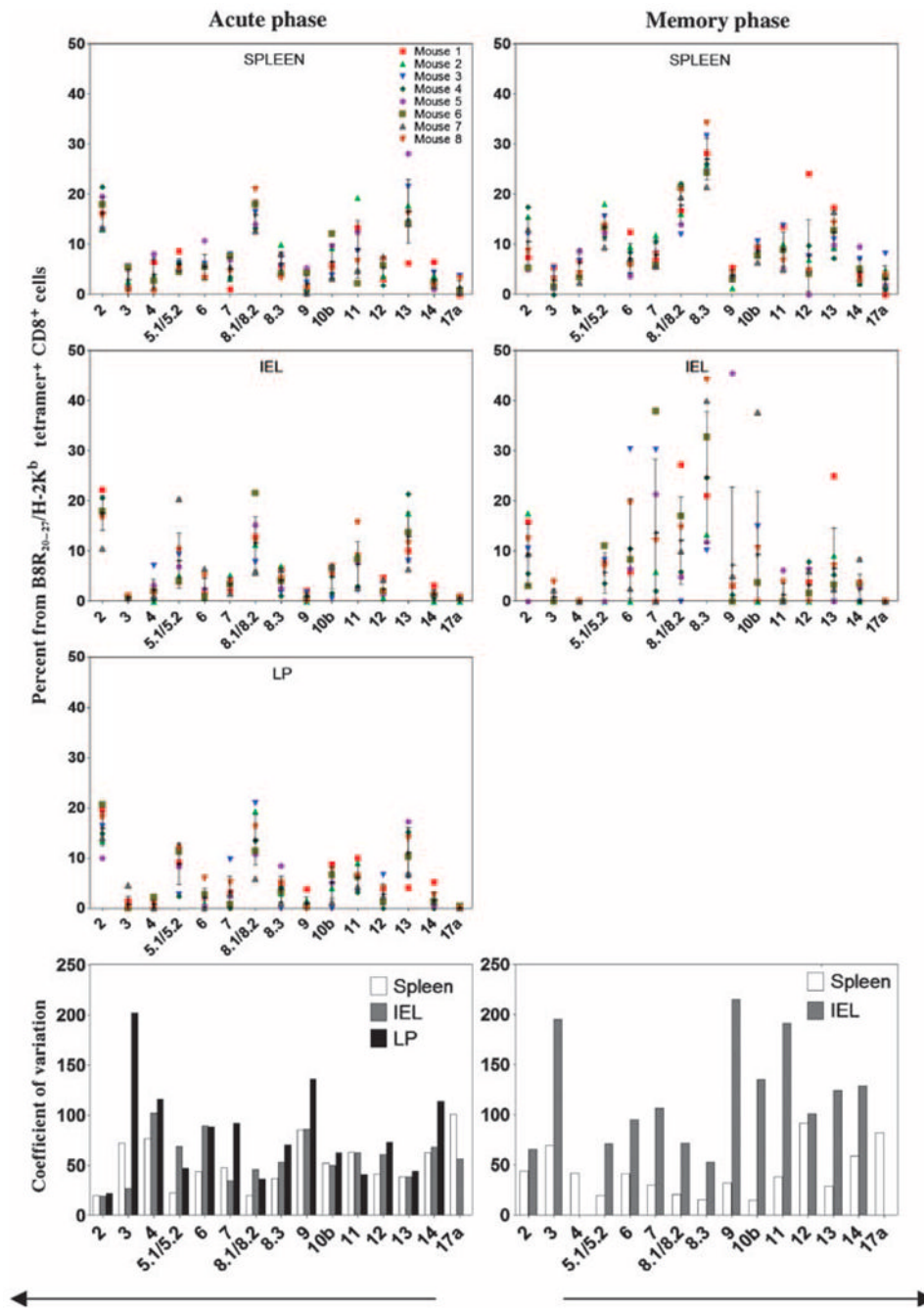


**Figure 3.** TCR V $\beta$ -chain profile expressed by B8R<sub>20-27</sub>/H2-K<sup>b</sup> tetramer<sup>+</sup> CD8<sup>+</sup> T cells in the spleen, SI-IEL, and SI-LP during acute and memory phases of MVA infection. (a and b) Lymphocytes from the spleen and small intestine were isolated from the spleen, SI-IEL, and SI-LP at acute (7 days) and memory (2 months) phases of MVA infection. Cells were stained with phycoerythrin-conjugated B8R<sub>20-27</sub>/H2-K<sup>b</sup> tetramer<sup>+</sup> and CD8 $\alpha$  mAbs and gated on tetramer<sup>+</sup> CD8 $\alpha$ <sup>+</sup> population. Then, additionally stained with anti-TCR V $\beta$ -chain mAbs, we assessed the relative percentage of each TCR V $\beta$ -chain inside gated cells. Data represent TCR V $\beta$ -chain profile in individual mice from two independent experiments (mean $\pm$ s.d.). (c and d) To measure the variation in a TCR V $\beta$ -chain data distribution in

different tissues in individual mice, we calculated coefficient of variation (CV) = s.d.×100%/mean value. A high CV corresponds to the high degree of variation in the sample. IEL, intraepithelial lymphocyte; LP, lamina propria; mAbs, monoclonal antibodies; MVA, Modified Vaccinia Ankara.

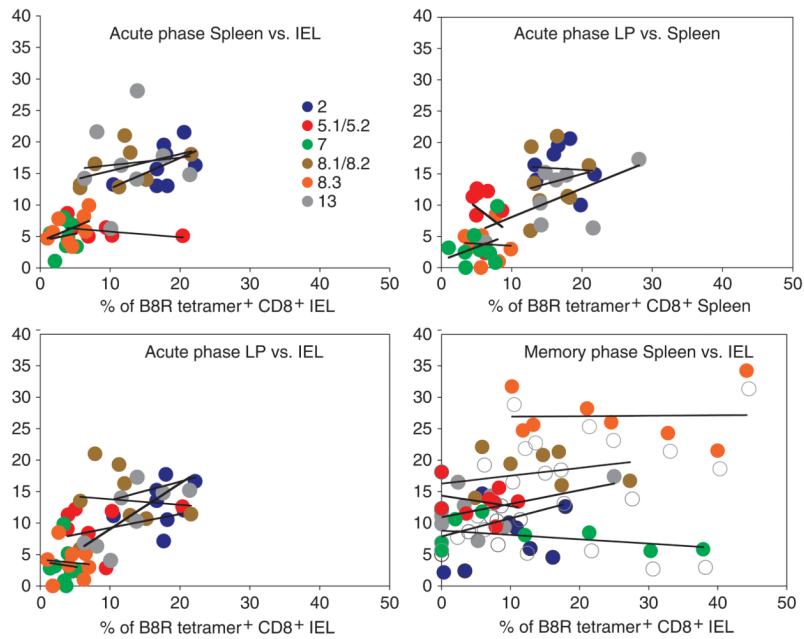


**Figure 4.**

Correlative analysis of TCR V $\beta$ -chain profile expressed by B8R<sub>20-27</sub>/H2-K<sup>b</sup> tetramer<sup>+</sup> CD8<sup>+</sup> T cells in the spleen, SI-IEL, and SI-LP at acute and memory phases of MVA infection. Selective correlative analysis for TCR V $\beta$ 2, -5.1/5.2, -7, -8.1/8.2, -8.3, and -13 chain carrier distribution. Data represent the original values shown on Figure 3a and b.

Acute phase: IEL vs. spleen: V $\beta$ 2 ( $R^2 = 0.2708$ ), V $\beta$ 5.1/5.2 ( $R^2 = 0.1392$ ), V $\beta$ 7 ( $R^2 = 0.0136$ ), V $\beta$ 8.1/8.2 ( $R^2 = 0.212$ ), V $\beta$ 8.3 ( $R^2 = 0.02099$ ), V $\beta$ 13 ( $R^2 = 0.0089$ ); IEL vs. LP: V $\beta$ 2 ( $R^2 = 0.0839$ ), V $\beta$ 5.1/5.2 ( $R^2 = 0.0849$ ), V $\beta$ 7 ( $R^2 = 0.0046$ ), V $\beta$ 8.1/8.2 ( $R^2 = 0.0091$ ), V $\beta$ 8.3 ( $R^2 = 0.0089$ ), V $\beta$ 13 ( $R^2 = 0.5364$ ); LP vs. spleen: V $\beta$ 2 ( $R^2 = 0.0039$ ), V $\beta$ 5.1/5.2 ( $R^2 = 0.0762$ ), V $\beta$ 7 ( $R^2 = 0.1109$ ), V $\beta$ 8.1/8.2 ( $R^2 = 0.0368$ ), V $\beta$ 8.3 ( $R^2 = 0.0032$ ), V $\beta$ 13 ( $R^2 = 0.3505$ ). Memory phase: IEL vs. spleen: V $\beta$ 2 ( $R^2 = 0.1447$ ), V $\beta$ 5.1/5.2 ( $R^2 = 0.0662$ ), V $\beta$ 7 ( $R^2 = 0.1825$ ), V $\beta$ 8.1/8.2 ( $R^2 = 0.087$ ), V $\beta$ 8.3 ( $R^2 = 0.0004$ ), V $\beta$ 13 ( $R^2 = 0.2366$ ). IEL, intraepithelial lymphocyte; LP, lamina propria; MVA, Modified Vaccinia Ankara.

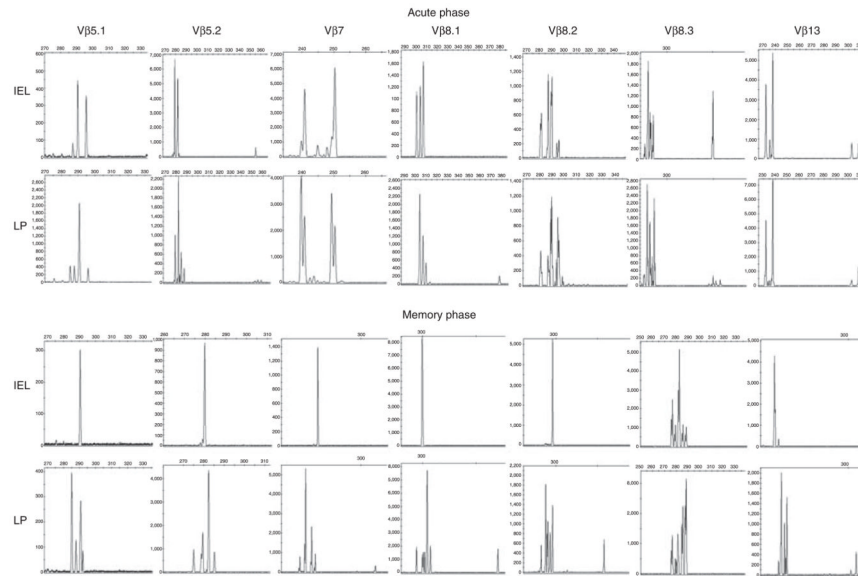


**Figure 5.** Immunoscope analysis of the B8R tetramer<sup>+</sup>-sorted CD8<sup>+</sup> T cells from IEL and LP compartments. CDR3 length analysis of the IEL and LP B8R tetramer<sup>+</sup> CD8<sup>+</sup>-sorted T cells from the same mouse is shown for d7 (acute phase) and d60 (memory phase) after infection. CDR3 analysis only for dominant Vβ-chain genes is shown. Strong oligoclonality is found in all samples. Memory B8R tetramer<sup>+</sup> CD8<sup>+</sup> IELs are represented by significantly fewer clones than memory LP T cells. Representative data of  $N = 4$  are presented. IEL, intraepithelial lymphocyte; LP, lamina propria.

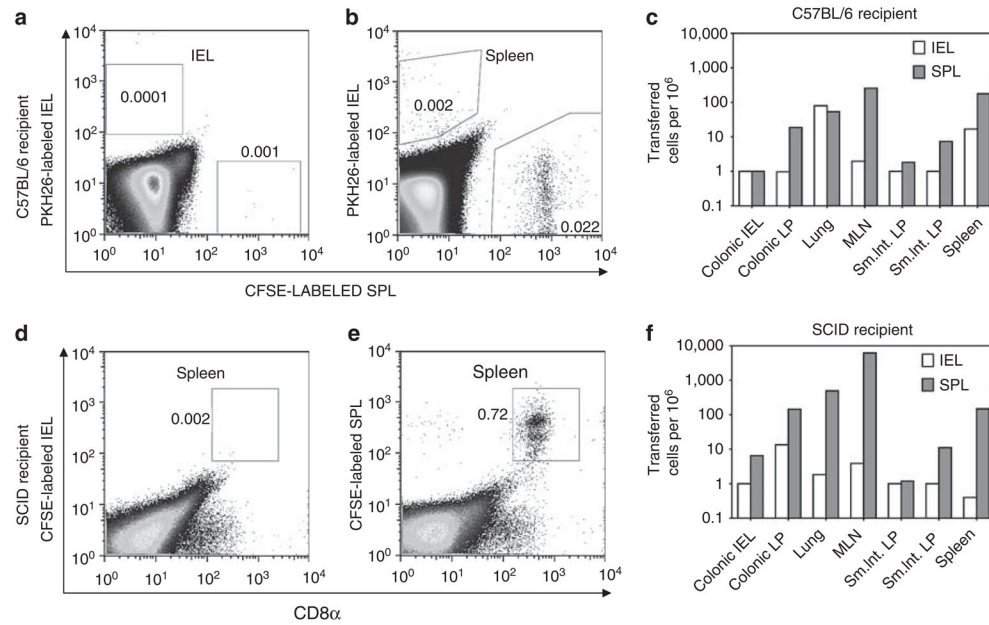


**Figure 6.**

Adoptively transferred CD8<sup>+</sup> IELs poorly migrate into small intestinal mucosa. **(a and b)** Lymphocytes from the spleen and IEL from naive donor C57BL/6 mice were isolated on CD8 magnetic beads (viability >99%), then CD8<sup>+</sup> IEL cells were labeled with red fluorescent linker, and splenocytes labeled with CFSE, mixed together at a 1:1 ratio, and total 5×10<sup>6</sup> CD8<sup>+</sup> T cells were transferred i.v. into naive wild-type mice. Twenty-four hours later, lymphocytes were isolated from the small intestine IEL **(a)** and LP, large intestine IEL and LP, mesenteric lymph nodes, spleen, **(b)** and lungs and analyzed by flow cytometry. **(c)** The number of donor spleen and IEL cells recovered in different tissues of recipient animals is shown. **(d and e)** Cells from naive donor C57BL/6 mice were isolated from IEL or spleen as described for **(a)** and **(b)**, labeled with CFSE, and separately transferred i.v. into naive recipient SCID mice. Seven days after the transfer, the presence of donor CFSE<sup>+</sup> IEL **(d)** or donor splenocytes **(e)** in the corresponding recipient tissue was analyzed by flow cytometry. **(f)** Number of donor spleen and IEL cells recovered in different tissues of recipient animals is shown. CFSE, carboxyfluorescein succinimidyl ester; IEL, intraepithelial lymphocyte; LP, lamina propria; SCID, severe combined immunodeficiency.